High energy green nanosecond and picosecond pulse delivery through a Negative Curvature Fiber for precision micro-machining

Piotr Jaworski,[1*] Fei Yu,[2] Richard M. Carter,[1] Jonathan C. Knight,[2] Jonathan D. Shephard,[1] and Duncan P. Hand[1]

[1] *Applied Optics and Photonics Group, Institute of Photonics and Quantum Sciences, Heriot-Watt University, Edinburgh, EH14 4AS, UK*

[2] *Centre for Photonics and Photonic Materials, Department of Physics, University of Bath, Bath, BA2 7AY, UK*

[*] *pj46@hw.ac.uk*

Abstract: In this paper we present an anti-resonant guiding, low-loss Negative Curvature Fiber (NCF) for the efficient delivery of high energy short (ns) and ultrashort (ps) pulsed laser light in the green spectral region. The fabricated NCF has an attenuation of 0.15 dB/m and 0.18 dB/m at 532 nm and 515 nm respectively, and provided robust transmission of nanosecond and picosecond pulses with energies of 0.57 mJ (10.4 kW peak power) and 30 μJ (5 MW peak power) respectively. It provides single-mode, stable (low bend-sensitivity) output and maintains spectral and temporal properties of the source laser beam. The practical application of fiber-delivered pulses has been demonstrated in precision micro-machining and marking of metals and glass.

OCIS codes: (060.0060) Fiber optics and optical communications; (060.4005) Microstructured fibers; (060.5295) Photonic crystal fibers; (060.2270) Fiber characterization; (140.3390) Laser materials processing.

References and links

1. K. L. Wlodarczyk and D. P. Hand, "Shaping the surface of Borofloat 33 glass with ultrashort laser pulses and a spatial light modulator," Appl. Opt. **53**(9), 1759-1756 (2014).
2. R. J. Beck, J. P. Parry, W. N. MacPherson, A. Waddie, N. J. Weston, J. D. Shephard, and D. P. Hand, "Application of cooled spatial light modulator for high power nanosecond laser micromachining," Opt. Express **18**(16), 17059-17065 (2010).
3. J. P. Parry, J. D. Shephard, M. J. Thomson, M. R. Taghizadeh, J. D. C. Jones, and D. P. Hand, "Optical fiber array for the delivery of high peak-power laser pulses for fluid flow measurements," Appl. Opt. **46**(17), 3432-3438 (2007).
4. P. J. Mosley, W. C. Huang, M. G. Welch, B. J. Mangan, W. J. Wadsworth, and J. C. Knight, "Ultrashort pulse compression and delivery in a hollow-core photonic crystal fiber at 540 nm wavelength," Opt. Lett. **35**(21), 3589-3591 (2010).
5. P. Jaworski, F. Yu, R. M. Carter, W. J. Wadsworth, T. A. Birks, J. C. Knight, J. D. Shephard, and D. P. Hand, "High peak power nanosecond and picosecond pulse delivery through a hollow-core Negative Curvature Fiber in the green spectral region for micro-machining," in *Advanced Photonics*, OSA Technical Digest (online) (Optical Society of America, 2014), paper SoM3B.5.
6. B. Debord, M. Alharbi, A. Benoit, D. Ghosh, M. Dontabactouny, L. Vincetti, J. -M. Blondy, F. Gerome, and F. Benabid, "Ultra low-loss hypocycloid-core Kagome hollow-core photonic crystal fiber for green spectral-range applications," Opt. Lett. **39**(21), 6245-6248 (2014).
7. A. Hartung, J. Kobelke, A. Schwuchow, K. Wondraczek, J. Bierlich, J. Popp, T. Frosch, and M. A. Schmidt, "Origins of modal loss of antiresonant hollow-core optical fibers in the ultraviolet," Opt. Express **23**, 2557-2565 (2015).
8. P. Jaworski, F. Yu, R. R. J. Maier, W. J. Wadsworth, J. C. Knight, J. D. Shephard, and D. P. Hand, "Picosecond and nanosecond pulse delivery through a hollow-core Negative Curvature Fiber for micro-machining applications," Opt. Express **21**(19), 22742-22753 (2013).
9. B. Beaudou, F. Gerome, Y. Y. Wang, M. Alharbi, T. D. Bradley, G. Humbert, J. -L. Auguste, J. -M. Blondy, and F. Benabid, "Millijoule laser pulse delivery for spark ignition through kagome hollow-core fiber," Opt. Lett. **37**(9), 1430-1432 (2012).

10. B. Debord, M. Alharbi, L. Vincetti, A. Huskaou, C. Fourcade-Dutin, C. Hoenninger, E. Mottay, F. Gerome, and F. Benabid, "Multi-meter fiber-delivery and pulse self-compression of milli-Joule femtosecond laser and fiber-aided laser-micromachining," Opt. Express **22**(9), 10735-10746 (2014).
11. P. Jaworski, F. Yu, D. G. MacLachlan, R. R. Maier, R. R. Thomson, W. J. Wadsworth, J. C. Knight, J. D. Shephard, and D. P. Hand, "A hollow-core Negative Curvature Fibre for efficient delivery of NIR picosecond and femtosecond pulses for precision micro-machining, " in *Workshop on Specialty Optical Fibers and their Applications*, (Optical Society of America, 2013), paper F3.3.
12. A. Urich, R. R. J. Maier, F. Yu, J. C. Knight, D. P. Hand, and J. D. Shephard, "Flexible delivery of Er:YAG radiation at 2.94 µm with negative curvature silica glass fibers: a new solution for minimally invasive surgical procedures," Biomed. Opt. Express **4**(2), 193-205 (2013).
13. F. Yu, W. J. Wadsworth, and J. C. Knight, "Low loss silica hollow core fibers for 3-4 µm spectral region," Opt. Express **20**(10), 11153-11158 (2012).
14. N. M. Litchinitser, A. K. Abeeluck, C. Headley, and B. J. Eggleton, "Antiresonant reflecting photonic crystal optical waveguides," Opt. Lett. **27**(18), 1592-1594 (2002).
15. J. D. Shephard, P. J. Roberts, J. D. C. Jones, J. C. Knight, and D. P. Hand, "Measuring beam quality of hollow core photonic crystal fibers," J. Lightwave Technol. **24**, 3761-3769 (2006).

1. Introduction

High energy laser pulses in the visible spectral range (in particular around 515 nm - 540 nm, where the neodymium and ytterbium based high-energy pulsed laser systems operate at their second harmonic wavelength), are extensively used in various applications including laser-machining and particle image velocimetry (PIV) [1-3]. For laser machining a key advantage of visible light compared with the fundamental NIR wavelengths is the focused spot size, enabling higher precision, and the more readily accessed non-linear absorption. PIV, meanwhile, requires a wavelength at which silicon-based cameras are suitably sensitive (i.e. visible rather than > 1µm). However the full range of potential applications of high pulse energy green light is limited by the lack of flexible beam delivery.

Conventional silica-based optical fibers cannot be used with such high pulse energies in the green because of their low damage threshold and strong nonlinearity. Furthermore hollow-core photonic crystal fibers (HC-PCFs), although providing excellent performance at wavelengths around 1µm, have limited use at shorter wavelengths due to increased scattering, and the lowest reported loss at 540 nm is 0.5 dB/m [4]. Hence an alternative technology – the anti-resonant guiding fiber – was developed for green light [5,6] and recently for ultraviolet (UV) [7], to extend the excellent results obtained with such a structure in the IR and Mid-IR spectral regions [8-13]. Two such designs are defined by having a negative curvature of the core wall (introduced to reduce coupling into the core wall and cladding structure). The first is more complex design consisting of a multiple layer photonic lattice known as the 'hypocycloid' Kagome fiber [9] and the second is a simpler 'negative curvature fiber' (NCF) [8] where the cladding is formed by a single ring of capillaries. These fibers have shown capacity to deliver picosecond pulses at 515 nm with average powers of 7.3 W (for the Kagome) and 6 W (for the NCF). The transmission of picosecond pulses through the NCF was limited by a non-optimized structure resulting in increased attenuation and instability (multimode behavior) of the delivered beam. The maximum delivered power in the ps pulse regime through the hypocycloid Kagome fiber was limited by the significant mismatch between coupling and fiber parameters which reduced transmission efficiency to approximately 60%.

In this paper we present an improved Negative Curvature Fiber for green light providing stable, single-mode output with lower attenuation than the previously published fiber and allowing transmission of ps pulses with significantly higher energy and average power than those reported in [6] for the Kagome hypocycloid structure.

2. Fiber characterization

2.1 Guidance in the visible spectral range

Light guidance in a Negative Curvature Fiber is described by the Anti-Resonant Reflecting Optical Waveguiding (ARROW) mechanism as explained in [14]. The presented NCF was fabricated using the conventional stack and draw technique. The parameters of the fabrication process were set to produce a uniform fiber structure with 122 µm outer diameter, 15 µm diameter hollow air core and a core wall thickness of approximately 550 nm (measurement uncertainty of 30 nm) which defines the guided wavelength range. The measured Mode Field Diameter (MFD) and NA of the fiber are 7.5 µm and 0.038 respectively. An SEM image of the fabricated fiber is shown in Fig. 1.

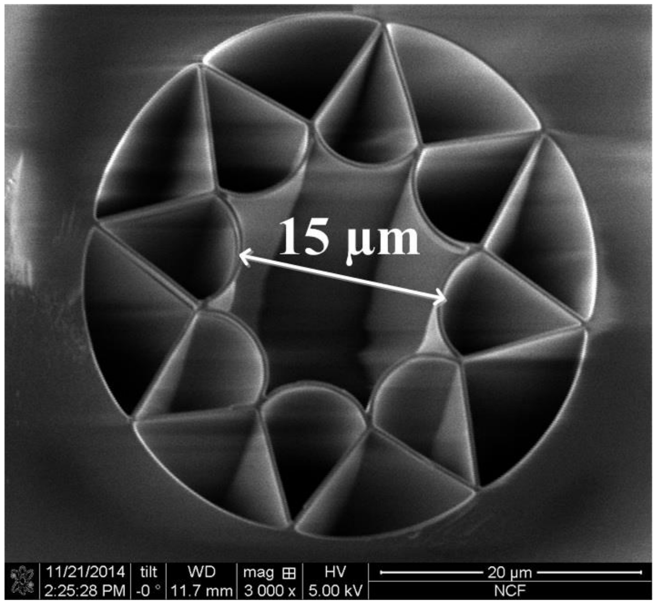

Fig. 1. SEM image of the fabricated NCF.

To determine the position of the low-loss guidance region, transmission measurements were made over a wide spectral range, from 400 nm to 650 nm, using a tungsten halogen lamp together with an Ando Optical Spectrum Analyzer AQ-6315B. To determine attenuation a standard cut-back technique was used, with the fiber cut from 40 m to 10 m without disturbing the coupling conditions. The results of transmission measurements, together with the calculated loss are presented in Figs. 2 and 3 respectively. The low-loss region covers a large part of the visible spectral range, spanning 120 nm (490 nm – 610 nm).

Additionally, to establish the attenuation of the NCF at 515 nm and 532 nm a series of cutback measurements was performed with coherent light sources. Two lasers, a Trumpf TruMicro picosecond system (515 nm, 6 ps) and a Spectra Physics Q-switched system (532 nm, 55 ns) were used. At both wavelengths the fiber attenuation was measured using the cut-back technique, in this case a straight 1 m length of fiber cut-back to 10 cm. The measured losses at 515 nm and 532 nm were at the level of 0.18 dB/m and 0.15 dB/m respectively. The results clearly indicate an improvement in guidance properties of the fiber at both wavelengths in comparison with the first fabricated "green" NCF [5] and are comparable with what is achievable with a Kagome-type hypocycloid hollow-core fiber [6].

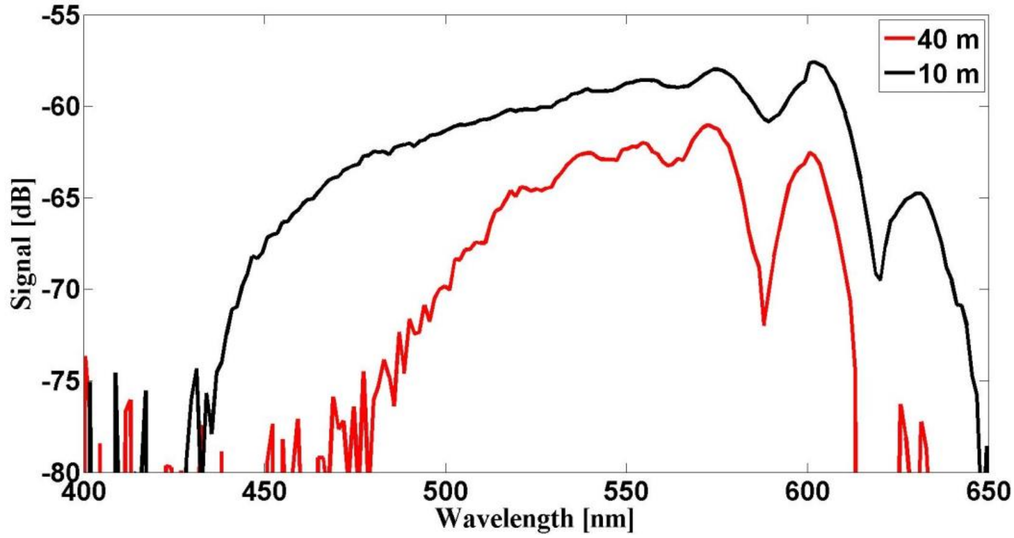

Fig. 2. Transmission spectra of 10 m (solid black line) and 40 m (solid red line) NCFs.

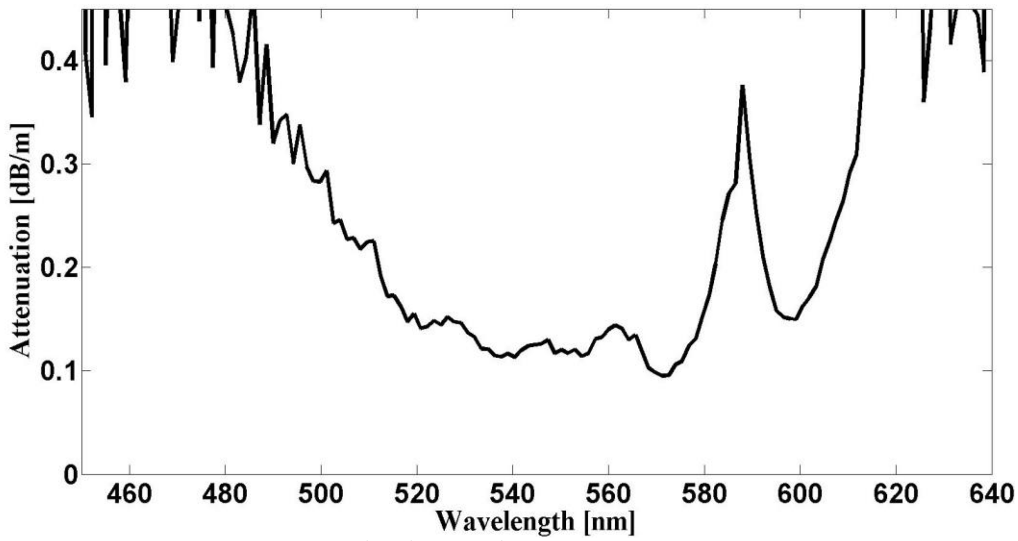

Fig. 3. Attenuation spectrum of the fabricated fiber.

2.2 Bending properties

The bending properties of the NCF, which determine its suitability for flexible beam delivery, were investigated at 532 nm and 515 nm. For measurements in this spectral region the Spectra Physics Q-switched Nd:YAG ns laser (532 nm) and Trumpf TruMicro thin disk ps laser (515 nm) were used.

The bend loss of the NCF was measured by bending a 1.2 m long fiber through 180° with bend diameters ranging from 25 cm to 1 cm (see Fig. 4) and comparing the transmitted power to the value delivered through a straight fiber. To obtain reliable results the coupling conditions for both straight and bent fibers were maintained during the entire experiment. Additionally the output of the NCF was characterized with a CCD camera and Spiricon beam analyzing software by capturing delivered beam patterns for each bend diameter. The measured bend loss and delivered beam profile changes at 532 nm and 515 nm are shown in Figs. 5, 6(a) and 6(b) respectively. Significant bend sensitivity was observed for bend radii below 2.5 cm, however at the larger bend diameters no impact on the transmitted power was detected. The NCF-delivered beam profiles show excellent stability with both lasers, indicating single-mode operation. No measurable difference in the delivered M^2 values was observed during fiber bending. However, the mode is closer to Gaussian and more symmetrical at 515 nm. Furthermore, the mode profile is circularly symmetric, in contrast to the hexagonal symmetry commonly seen with typical HC-PCFs [15], potentially providing improvement to micro-machining processes.

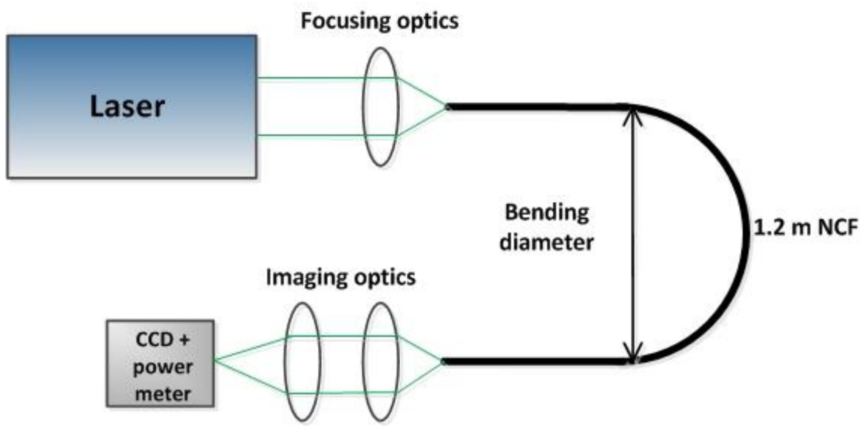

Fig. 4. Experimental setup for fiber bending tests.

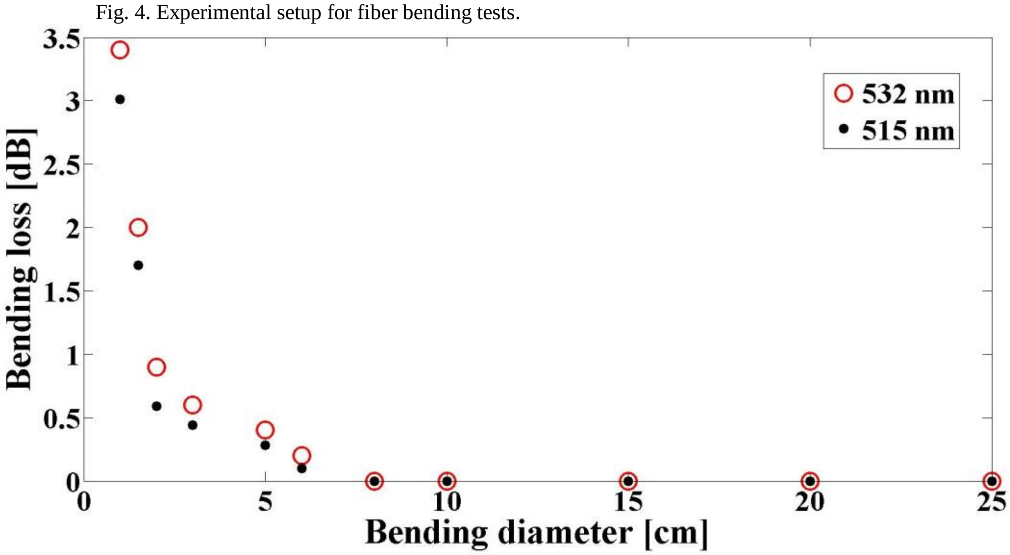

Fig. 5. Bending loss present in 1.2 m fiber due to 180° bend for different bending diameters at 532 nm (red circles) and 515 nm (black dots).

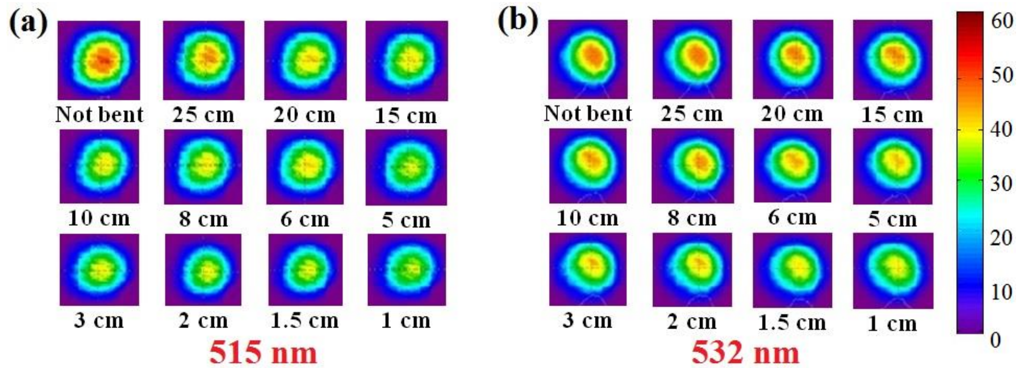

Fig. 6. NCF-delivered beam profiles for different bend diameters at: (a) 515 nm; (b) 532 nm. Note that the distortions (fringes) visible in the beam patterns are due to interference from the filters used in the imaging system.

3. High peak power pulse delivery

3.1 Nanosecond pulse delivery

Fiber power handling experiments were performed with two lengths of fiber, (i) short, 1.2 m (straight), and (ii) long, 8.8 m (coiled on a drum with 15 cm coil diameter), with the same laser as used with the transmission and bend loss measurements. A plano-convex lens of focal length 15 mm was used to provide optimal laser beam to fiber coupling. This provided a spot diameter of 8.5 µm ($1/e^2$) with a focus cone angle of 0.038 rad, enabling a 91.5% launch efficiency and excitation of the fundamental mode only (presence of the higher order modes was not observed). No fiber damage was observed even when coupling the maximum laser power into 1.2 m NCF, providing a maximum delivered average power of 8.6 W with 0.57 mJ pulse energy and 10.4 kW peak power. The corresponding peak power density and energy density reached 23.6 $GWcm^{-2}$ and 1290 Jcm^{-2} respectively. The 8.8 m long coil of fiber was also undamaged by the maximum available laser power, delivering a pulse energy of 0.44 mJ, average power of 6.6 W and a peak power of 8 kW. Unfortunately a high power ns source was not available, so it was not possible to establish the ultimate damage limitation with this pulse length. To determine the quality of the delivered beam the end-facet of the NCF was directly imaged (and magnified) onto a CCD camera connected with Spiricon beam profiling software and the M^2 parameter was measured using the ($1/e^2$) criteria to define beam width. The near-field NCF-delivered beam profile with 7.5 µm diameter ($1/e^2$ value corresponding to the MFD of the NCF) is shown in Fig. 7(a) (the distortions present in the image are due to interference features from the filters used in the imaging system, rather than the excitation of the higher order modes). The measured M^2 value of the delivered beam was 1.36 as shown in Fig. 7(b).

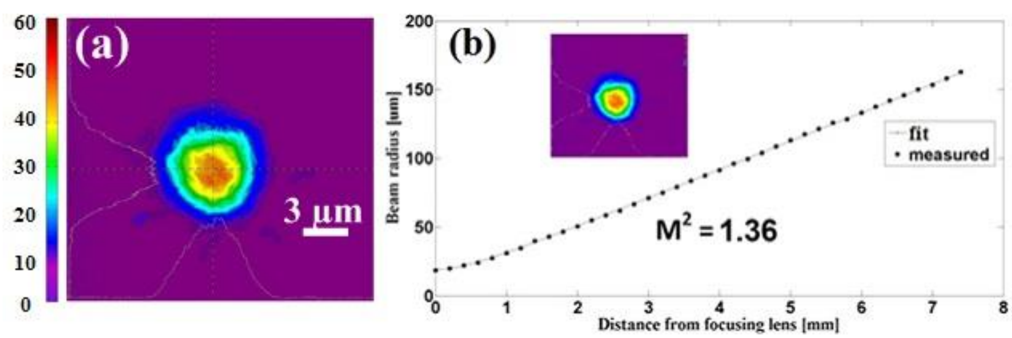

Fig. 7. (a) Fiber-delivered near field beam profile. (b) Results of the M^2 measurement of the fiber-delivered beam at 532 nm.

3.2 Picosecond pulse delivery

Light from the Trumpf ps laser was coupled into the NCF core using a plano-convex lens of focal length 35 mm to generate an 8.0 µm diameter ($1/e^2$) spot and a focus cone angle of 0.042 rad. A slight mismatch with the acceptance angle of the fiber meant that the maximum coupling efficiency that could be obtained in this case was 90%. The maximum delivered pulse energy through a 1 m length of NCF without damage was 30 µJ (35 µJ coupled) with an average power of 12 W (13.9 W coupled) and 5 MW peak power which corresponds to energy and peak power densities of 68 Jcm^{-2} and 11.3 $TWcm^{-2}$ respectively. This delivered average power was twice that previously reported with a Kagome hypocycloid hollow-core fiber [6]. To determine the damage threshold of the NCF the amount of coupled pulse energy was slowly increased (while maintaining the same coupling efficiency) until a failure occurred. Damage to the input end-facet of the fiber was observed for pulse energies of 40 µJ, which corresponds to energy density of 80 Jcm^{-2}.

When an ultrashort pulse is transmitted through a hollow-core fiber its temporal properties could be affected by the presence of higher order modes, which typically causes pulse broadening as a result of intermodal dispersion, as well as by the presence of waveguide dispersion of the fundamental mode. Furthermore, due to a mismatch with the acceptance angle of the fiber, light could be coupled into the cladding causing generation of additional wavelengths due to nonlinear effects in the silica glass which significantly alters the spectrum of the delivered pulse. In order to investigate the impact of the fiber on the spectral and temporal properties of the laser pulses an Ocean Optics spectrometer (0.05 nm FWHM spectral resolution) and an APE PulseCheck autocorrelator were used. The recorded spectra of the beam directly from the laser and after propagation through 1 m and 8.8 m lengths of NCF are shown in Fig. 8. The results clearly show that the shape of the optical spectrum of the laser was well maintained through both fiber lengths, with no additional wavelengths generated, indicating an absence of nonlinear effects. The intensity autocorrelation traces of the delivered pulses shown in figure 9 confirm this, with no changes in shape and no broadening in comparison with original laser pulse. This demonstrates the suitability of the NCF for efficient transmission of ultrashort pulsed laser light.

The near-field NCF-delivered beam profile was captured with a CCD camera and Spiricon software as shown in Fig. 10(a). As with the ns case, the M^2 parameter was also determined by imaging a number of planes, and found to be 1.33 (see Fig. 10(b)), which is comparable with the ns results.

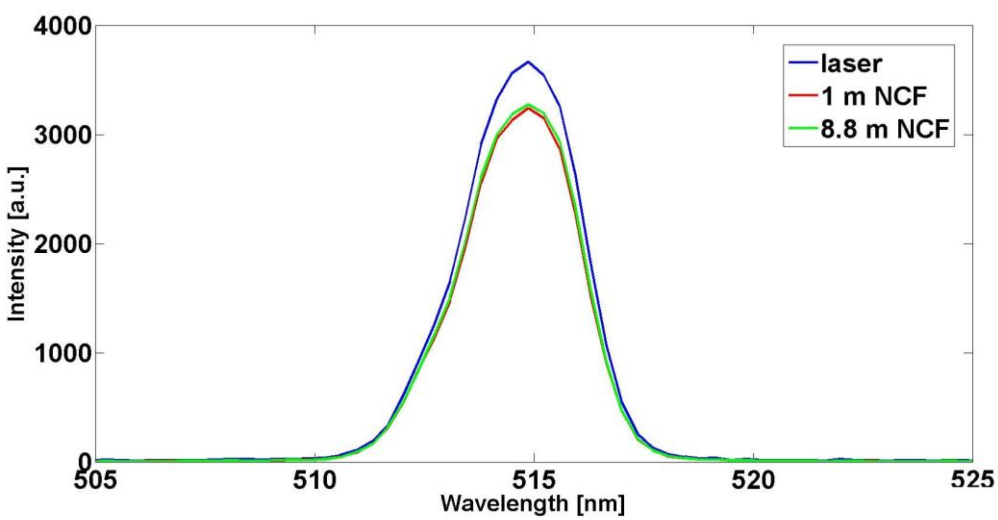

Fig. 8. Optical spectra of: picosecond laser beam (35 µJ pulse energy, solid blue line); delivered beam through 1 m NCF (30 µJ pulse energy, solid red line) and 8.8 m NCF (21.5 µJ pulse energy, solid green line).

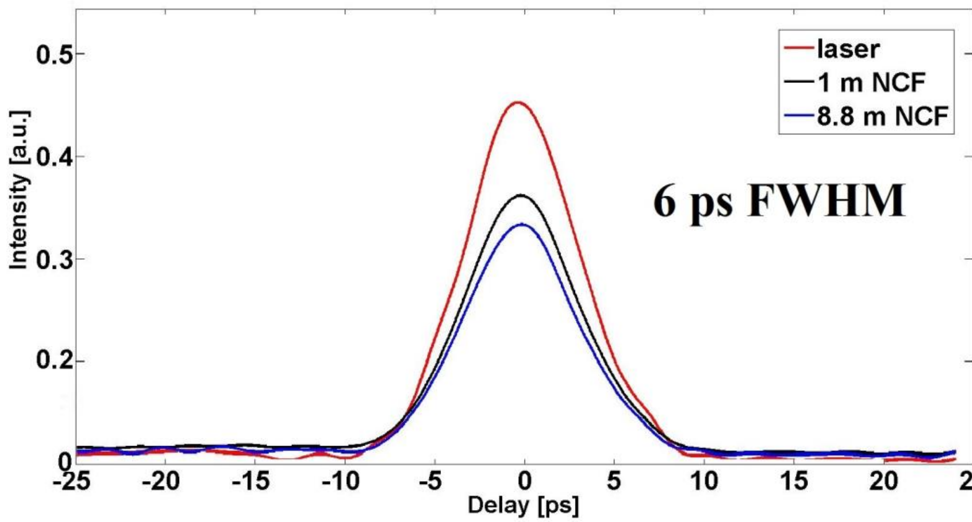

Fig. 9. Intensity autocorrelation traces of: picosecond laser light (35 µJ, solid red line); transmitted beam through 1m fiber (30 µJ, solid black line) and 8.8 m NCF (21.5 µJ, solid blue line).

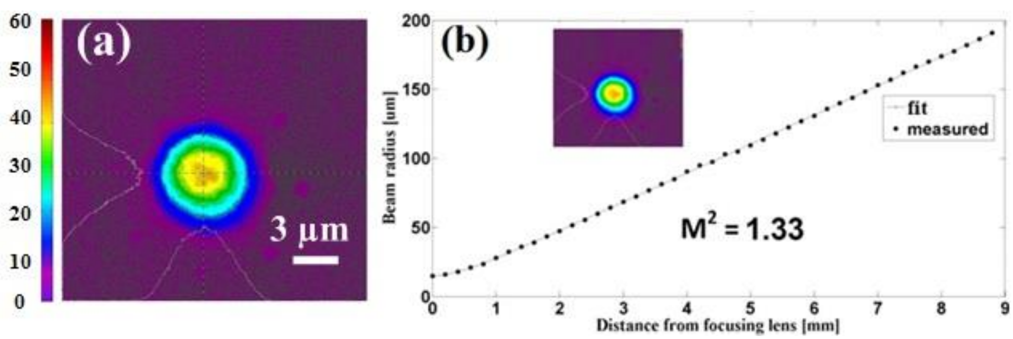

Fig. 10. (a) NCF-delivered near field beam profile. (b) Beam radius measurements and M^2 parameter fit of the fiber-delivered beam at 515 nm.

4. Example application of NCF-delivered laser light: marking and micro-machining

4.1 Nanosecond and picosecond marking and micro-machining of different materials

Example applications with the NCF-delivered green pulses were demonstrated, namely through cutting aluminum sheet and marking titanium with the ns system, and micro-milling fused silica with the ps laser. In both cases, the laser beam was delivered through the fiber to galvanometer scan head systems fitted with f-theta lenses with focal lengths of 125 mm and 163 mm for the ns and ps lasers respectively, providing focused spot diameters on the machined sample of approximately 25 µm and 28 µm ($1/e^2$ values, calculated).

To perform both through cutting of 0.3 mm thick aluminum sheet and marking in titanium, identical ns pulse energies and repetition rates were used; 0.35 mJ and 15 kHz. The scan speed, however, was optimized to 0.1 mm/s and 100 mm/s for cutting and marking respectively. In both cases this allowed high quality features to be fabricated without introducing any damage to the surrounding material, as shown in Figs. 11(a) and 11(b).

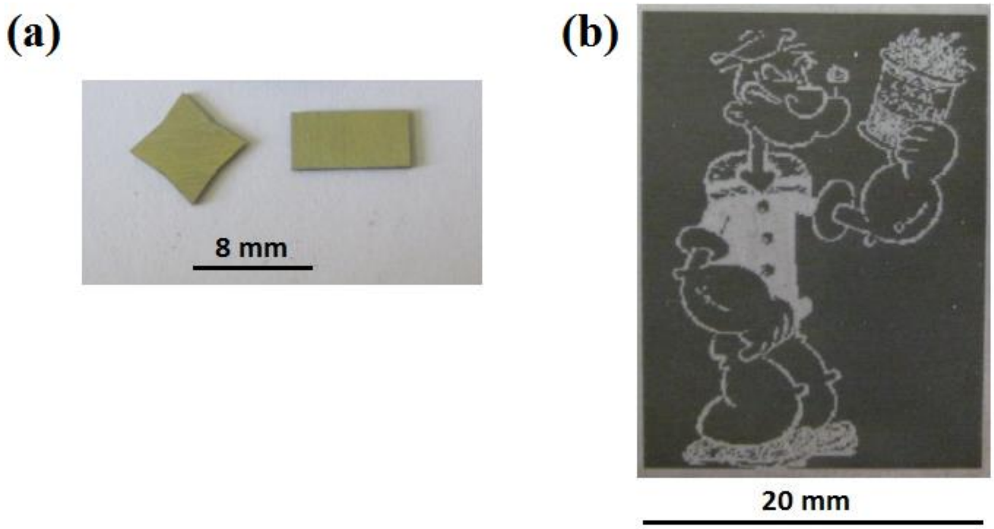

Fig. 11. Results of ns machining with NCF-delivered pulses: (a) cutting of aluminum; (b) marking in titanium.

Pulses delivered from the ps laser (14 µJ, 400 kHz) were used to micro-mill fused silica. The machining speed was set to 1 mm/s. The excellent beam quality provided by the fiber allowed high quality, small features to be fabricated (down to 0.4 mm by 0.4 mm) without creating any cracks on either the machined or surrounding area of the glass sample. Example structures are shown in Fig. 12.

Fig. 12. Examples of crack-free micro-milling of fused silica with NCF-delivered ps pulses.

5. Conclusions

In this paper we have reported a low-loss Negative Curvature Fiber for the flexible delivery of high energy nanosecond and picosecond pulses in the green spectral region for various micro-machining applications. The fabricated fiber can transmit 6 ps pulses with a maximum energy of 30 µJ and an average power of 12 W at 515 nm (average power more than double that previously reported in [6]). The NCF provides a stable single-mode output, with very low bend-sensitivity, and it does not degrade the temporal and spectral properties of the guided beam. Furthermore, the delivered light is suitable for precision micro-machining systems. The combination of a high-quality NCF-delivered beam and sufficient pulse energy allowed very high quality features to be generated in aluminum, titanium and fused silica.

Acknowledgments

This work is funded by the UK Engineering and Physical Sciences Research Council under grants EP/I01246X/1 and EP/I011315/1. The authors would like to acknowledge Renishaw plc for providing additional funding support.